PNAS RESEARCH ARTICLE | CELL BIOLOGY

Disassembly of bundled F-actin and cellular remodeling via an interplay of Mical, cofilin, and F-actin crosslinkers

Sudeepa Rajan[a,1], Jimok Yoon[b,c,1], Heng Wu[b,c], Sargis Srapyan[d], Raju Baskar[b,c], Giasuddin Ahmed[b,c], Taehong Yang[b,c], Elena E. Grintsevich[a,d,2], Emil Reisler[a,e,2], and Jonathan R. Terman[b,c,2]

Edited by David Drubin, University of California, Berkeley, CA; received June 16, 2023; accepted August 11, 2023

Cellular form and function are controlled by the assembly and stability of actin cytoskeletal structures—but disassembling/pruning these structures is equally essential for the plasticity and remodeling that underlie behavioral adaptations. Importantly, the mechanisms of actin assembly have been well-defined—including that it is driven by actin's polymerization into filaments (F-actin) and then often bundling by crosslinking proteins into stable higher-order structures. In contrast, it remains less clear how these stable bundled F-actin structures are rapidly disassembled. We now uncover mechanisms that rapidly and extensively disassemble bundled F-actin. Using biochemical, structural, and imaging assays with purified proteins, we show that F-actin bundled with one of the most prominent crosslinkers, fascin, is extensively disassembled by Mical, the F-actin disassembly enzyme. Furthermore, the product of this Mical effect, Mical-oxidized actin, is poorly bundled by fascin, thereby further amplifying Mical's disassembly effects on bundled F-actin. Moreover, another critical F-actin regulator, cofilin, also affects fascin-bundled filaments, but we find herein that it synergizes with Mical to dramatically amplify its disassembly of bundled F-actin compared to the sum of their individual effects. Genetic and high-resolution cellular assays reveal that Mical also counteracts crosslinking proteins/bundled F-actin in vivo to control cellular extension, axon guidance, and Semaphorin/Plexin cell-cell repulsion. Yet, our results also support the idea that fascin-bundling serves to dampen Mical's F-actin disassembly in vitro and in vivo—and that physiologically relevant cellular remodeling requires a fine-tuned interplay between the factors that build bundled F-actin networks and those that disassemble them.

MICAL1 | MICAL2 | MICAL3 | bristle | nervous system

Cellular form and function are governed through both stabilizing and destabilizing the actin cytoskeleton. In particular, actin's transition from monomeric (G-actin) to filamentous (F-actin) states—and then further transition into more stable structures of numerous bundled filaments, provides the stability essential for diverse cellular and tissue actions (1, 2). Importantly, an in-depth understanding has now been gained into how actin polymerizes and is organized into stable bundled F-actin networks, including the identification of numerous actin crosslinking/bundling proteins such as fascin, fimbrin, filamin, villin, α-actinin, and espin (1–3). In contrast, how these stable bundled F-actin structures are rapidly destabilized/disassembled remains less clear (2, 4, 5).

Recently, we defined a class of F-actin disassemblers—the MICALs [composed of one invertebrate (Mical) and three vertebrate (MICAL-1, MICAL-2, and MICAL-3) family members]—that regulates diverse cellular events in multiple tissues (6, 7). MICALs are oxidation-reduction (Redox) enzymes that directly bind to and are activated by F-actin. In the presence of their coenzyme (NADPH), MICALs promote F-actin disassembly [Fig. 1*A* (1 and 2); (8–11)]. MICALs disassemble F-actin through a catalytic posttranslational mechanism, directly oxidizing actin's methionine (M) M44 and M47 residues to destabilize filaments [Fig. 1*A* (2); (8–12)]. Previous work on MICALs has focused on its direct effects on unbundled filaments (6, 7), but observations indicated that MICALs also directly affect bundled filaments (8). In this regard, previous research has noted differences in the ability of the best-known disassembly proteins to disassemble bundled F-actin (e.g., refs. 2 and 13–18). This raised questions that we have pursued herein about the mechanisms by which the higher-order bundled F-actin structures that underlie cellular stability are rapidly disassembled/pruned to allow for cellular plasticity and remodeling.

Utilizing fascin, one of the most abundant F-actin-bundling proteins (19–23), our biochemical and real-time imaging results now show that in a similar way to unbundled filaments, the enzymatic activity of Mical is rapidly triggered by fascin-bundled F-actin, which it then oxidizes and extensively disassembles. Cofilin, a key F-actin severing and depolymerization factor, also affects fascin-bundled filaments (13), but we show herein

Significance

Organism form and behavior is governed by the basic building blocks of cellular structure, the actin cytoskeleton. Namely, actin proteins assemble into polymers (F-actin)—which are often transformed into complex bundled F-actin structures to enhance cellular stability. Yet, while we have an in-depth understanding of how actin polymerizes and is organized into bundled F-actin networks, how these stable bundles are rapidly pruned/disassembled to trigger changes to cellular form and function is less clear. Here, we uncover specific mechanisms of rapid disassembly of bundled F-actin to drive cellular shape and behavioral changes. Our observations also reveal a fine-tuned coordination between the building and breaking down of bundled F-actin networks with ramifications for governing normal to disease-state transitions.

Author contributions: S.R., J.Y., H.W., S.S., R.B., G.A., T.Y., E.E.G., E.R., and J.R.T. designed research; S.R., J.Y., H.W., S.S., R.B., G.A., T.Y., E.E.G., and J.R.T. performed research; S.R., J.Y., H.W., S.S., R.B., E.E.G., and J.R.T. contributed new reagents/analytic tools; S.R., J.Y., H.W., S.S., R.B., G.A., T.Y., E.E.G., E.R., and J.R.T. analyzed data; and S.R., J.Y., S.S., R.B., E.E.G., E.R., and J.R.T. wrote the paper.

The authors declare no competing interest.

This article is a PNAS Direct Submission.

[1]S.R. and J.Y. contributed equally to this work.

[2]To whom correspondence may be addressed. Email: elena.grintsevich@csulb.edu, reisler@mbi.ucla.edu, or jonathan.terman@utsouthwestern.edu.

This article contains supporting information online at https://www.pnas.org/lookup/suppl/doi:10.1073/pnas.2309955120/-/DCSupplemental.

Published September 19, 2023.

that Mical and cofilin synergize to dramatically amplify their individual rates and extent of bundled F-actin disassembly. Our results also show that Mical—in combination with cofilin—also disassembles bundled F-actin in vivo, but bundling proteins serve to dampen this effect to allow for proper cellular extension and Semaphorin/Plexin repulsive axon guidance.

Results

Mical Rapidly and Extensively Dismantles Bundled F-actin. Actin bundling/crosslinking proteins stabilize actin cytoskeletons by bundling together multiple single filaments (Fig. 1*B*). Yet, how these stable bundled F-actin structures are rapidly dismantled is yet to be clarified. Utilizing as a model the prominent and widely-expressed F-actin bundler fascin (19–23), we initiated experiments to further explore and quantify Mical's direct effects on bundled F-actin. First, consistent with previous observations using low-speed actin pelleting assays (8)—in which filaments predominantly remain in the supernatant unless bundled by fascin—we found that purified fascin robustly bundled F-actin (*SI Appendix*, Fig. S1 *A* and *B*), but purified Mical with its coenzyme NADPH, markedly reduced the amount of this pelleted (bundled) F-actin (*SI Appendix*, Fig. S1*C*). Following up on these observations, we found that even at saturating concentrations of fascin, Mical/NADPH markedly decreased bundled F-actin—and did so in a dosage-sensitive manner (Fig. 1*C* and *SI Appendix*, Fig. S1*D*). Moreover, light scattering measurements—to examine Mical's direct effects on bundled F-actin in real-time—revealed that Mical/NADPH rapidly and extensively disassembled fascin-bundled F-actin (Fig. 1*D* and *SI Appendix*, Fig. S1 *E* and *F*).

Because bundles are heterogeneous structures, bulk assays reveal only their average overall changes. We therefore next examined this Mical/NADPH-mediated bundled F-actin disassembly at the single molecular level using TIRF microscopy. Bundles were assembled on slide surfaces and exposed to Mical/NADPH. The images shown in Fig. 1*E* originated from representative movies (Movies S1–S3), and at the starting point of the recordings (after 14 min of on-slide polymerization and 2 to 3 min of Mical/NADPH treatment), the average bundle thickness was 3 to 4 filaments (ranging from 2 to 8). Notably, we observed that Mical/NAPDH markedly disassembled bundled F-actin (Fig. 1*E* (1); Movies S1–S3). Furthermore, fluorescence intensity analysis revealed two predominant modes by which Mical/NADPH induced the disassembly of fascin-bundled F-actin—receding and peeling/thinning modes (Fig. 1 *F* and *G*). Specifically, we defined bundle shortening without a change in maximal thickness as a "receding mode" of disassembly (Fig. 1*F*). We also observed bundle shortening accompanied by thinning (usually from one end) and defined it as a "thinning/peeling mode" of disassembly (Fig. 1*G*). Thus, different assays reveal that Mical/NADPH efficiently disassembles fascin-bundled F-actin.

Mical-Oxidized Actin Has a Reduced Ability to Form Bundled Filaments. Mical Redox enzymes catalyze the site-specific posttranslational modification (oxidation) of actin at its methionine (M) 44 and M47 residues [Fig. 1*A*; (9)]. The resulting Mical-oxidized actin (Mox-actin) can then be used to evaluate the effects of this oxidation on F-actin and its regulators (9, 10, 12, 24, 25). Notably, the "thinning/peeling mode" of bundled F-actin disassembly could indicate a reduced ability of fascin to bundle Mox-actin, resulting in "unzipping" of Mical-oxidized filaments from bundle surfaces. Therefore, to gain additional insight into Mical's effect on bundled F-actin, we examined fascin's ability to interact with Mox-F-actin, using Mox-actin at concentrations above its critical concentration of polymerization (>~1 μM) (10, 24, 25). Notably, using high-speed pelleting (binding) assays, only a marginal difference—if any—was observed between the binding affinity (K_{app}) of fascin to F-actin and Mox-F-actin (*SI Appendix*, Fig. S2 *A* and *B*). In contrast, using low-speed pelleting (bundling) assays, we found that unlike with unmodified F-actin, the majority of Mox-F-actin remained in the supernatant (i.e., unbundled) even at high fascin concentrations (Fig. 2*A* and *SI Appendix*, Fig. S1*B*). Fascin addition to Mox-F-actin also generated relatively small light scattering increases (i.e., less bundling), including >~fourfold smaller effects than when added to unmodified F-actin (Fig. 2 *B–D* and *SI Appendix*, Fig. S2 *C* and *D*). Moreover, observing F-actin and fascin-bundled F-actin using electron microscopy (EM) revealed that unmodified actin formed numerous, long, thick, and stereotypic tightly-adhered parallel bundles of approximately 5 to 10 filaments/bundle (Fig. 2 *E* and *F*). In contrast to that, Mox-F-actin and fascin formed fewer, shorter, and thinner bundles (2 to 4 filaments/bundle) that were often not tightly bundled together (Fig. 2 *G* and *H* and *SI Appendix*, Fig. S2 *E–H*). So too, unmodified actin was predominantly bundled (Fig. 2*F*), but Mox-F-actin remained mostly unbundled and/or formed aggregates of various disordered sizes, shapes, and incoherent/disorganized structures (Fig. 2*H* and *SI Appendix*, Fig. S2 *H–J*). Thus, different experimental approaches demonstrate that Mical's oxidation of actin has a negative effect on its bundling by fascin.

Fascin-Bundled F-actin Activates Mical's Catalytic F-actin Disassembly Effects. Our results reveal that Mical reduces bundled F-actin levels by both breaking-down existing fascin-bundled filaments and limiting their assembly. We next explored the mechanisms underlying Mical-induced disassembly of fascin-bundled F-actin. Notably, Mical does not itself bundle F-actin, nor does it alter fascin's ability to bundle unmodified F-actin (8). We therefore wondered if similar to unbundled F-actin, Mical is activated by fascin-bundled F-actin and modifies F-actin within it. First, we looked at fascin-bundled filaments' ability to activate Mical's enzymatic activity (via NADPH consumption). In particular, in the absence of a substrate, Mical consumes its coenzyme NADPH at a slow rate [Fig. 3*A*, green; (9, 11, 24)]. Adding fascin alone did not increase Mical's NADPH consumption rate (Fig. 3*A*, purple, and *SI Appendix*, Fig. S3 *A* and *B*), showing that fascin itself is not a direct Mical substrate. Fascin-bundled filaments, however, in a similar way to unbundled F-actin, strongly enhanced Mical-mediated NADPH consumption (Fig. 3*A*, blue, and *SI Appendix*, Fig. S3 *A* and *B*) in a bundled F-actin concentration-dependent manner (Fig. 3*B*). Next, we wondered whether fascin-bundled F-actin is oxidized by Mical. To identify this, limited subtilisin proteolysis assays have been used, which take advantage of subtilisin's inability to cleave Mical-oxidized actin between its M47 and G48 residues (24, 25). Notably, subtilisin assays revealed that F-actin bundled by fascin is indeed oxidized by Mical (Fig. 3 *C*, *Upper*). Furthermore, an antibody that recognizes the oxidized M44 residue of actin ($actin^{MetO44}$) (24) confirmed that Mical oxidizes fascin-bundled F-actin (Fig. 3*D*). Moreover, utilizing limited trypsin proteolysis assays to probe for Mical oxidation-induced structural alterations in F-actin revealed that fascin-bundled F-actin [similar to unbundled F-actin (26)] is resistant to tryptic digestion, but its treatment with Mical/NADPH accelerated tryptic digestion by ~fivefold (*SI Appendix*, Fig. S3*C*). Thus, both unbundled and fascin-bundled F-actin are utilized by Mical as a substrate, which Mical oxidizes to destabilize and eventually disassemble them.

Fascin's Bundling of F-actin Regulates Mical's Enzymatic Activity, Actin Oxidation, and F-actin Disassembly. We also noticed that compared to unbundled F-actin, fascin-bundled F-actin reduced

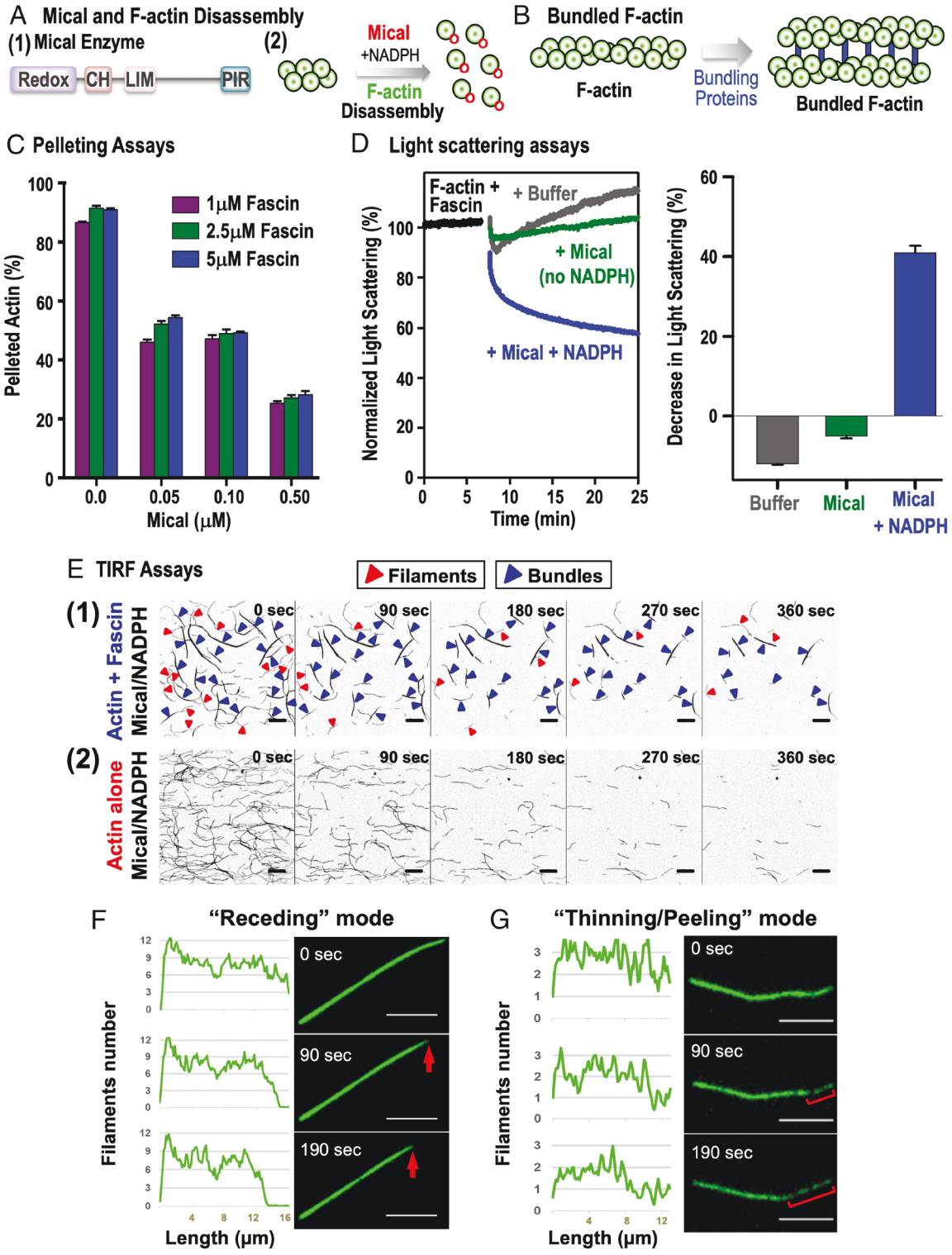

Fig. 1. Mical robustly disassembles fascin-bundled F-actin. (*A*) Mical and its effects on F-actin. (1) Mical enzyme. Redox enzymatic, CH (calponin homology), LIM (Lin11, Isl-1, and Mec-3), and PIR (Plexin-interacting region) domains. (2) Mical in the presence of its coenzyme NADPH disassembles F-actin (green) by oxidizing (red O) it. (*B*) Actin bundling/crosslinking proteins bundle actin together in different organizations, such as parallel-arranged filaments. (*C*) Pelleting assays show that Mical disassembles fascin-bundled F-actin at different saturating concentrations of fascin and in a Mical concentration-dependent manner. See *SI Appendix*, Fig. S1*D* for gels. [F-actin] = 5 μM, [NADPH] = 400 μM. [Mical], [fascin] as indicated. n = 3 independent experiments/condition. Mean ± SEM. (*D*) Light scattering assays show that Mical/NADPH disassembles fascin-bundled F-actin. Normalized light (325 nm) scattering percentage (%) changes [also for Figs. 2 *B* and *C* and 4*A* (1) and *SI Appendix*, Figs. S1 *E* and *F*, S2*D*, and S3*I*]. Specifically, F-actin was bundled with fascin to a steady state (black), and then buffer with NADPH (gray), Mical (green), or Mical with NADPH (blue) was added to it. [F-actin] = 5 μM, [fascin] = 5 μM, [Mical] = 0.05 μM, and [NADPH] = 100 μM. A representative experiment is shown (*Left*). n = 3 independent experiments/condition. Mean ± SEM. Minutes (min). (*E*) F-actin disassembly with (1) or without (2) fascin upon on-slide Mical/NADPH oxidation. Representative TIRFM movie montages; bar = 10 μm. Red and blue arrowheads indicate unbundled and bundled filaments, respectively. Seconds (sec). (*F* and *G*) Predominant modes of Mical-mediated bundled-F-actin disassembly observed by TIRFM. (*Left*) fluorescence intensity profiles of bundles from indicated time points and corrected for photobleaching: average fluorescence intensities of unbundled filaments from same movies (internal controls) were used to determine filaments number/bundle (Y-axes). (*Right*) representative TIRFM movie montages; bar = 5 μm. (*F*) "Receding mode" is defined as bundle shortening (red arrow) without changing its maximal thickness. (*G*) "Thinning/Peeling mode" is defined as bundle shortening accompanied by its thinning (usually from one end). Red bracket = thinning region. Note that bundle ends can alternate between "receding" and "thinning/peeling" disassembly modes. [actin] = 1.24 μM; [fascin] = 0.8 μM; [Mical] = 10 nM; [NADPH] = 100 μM.

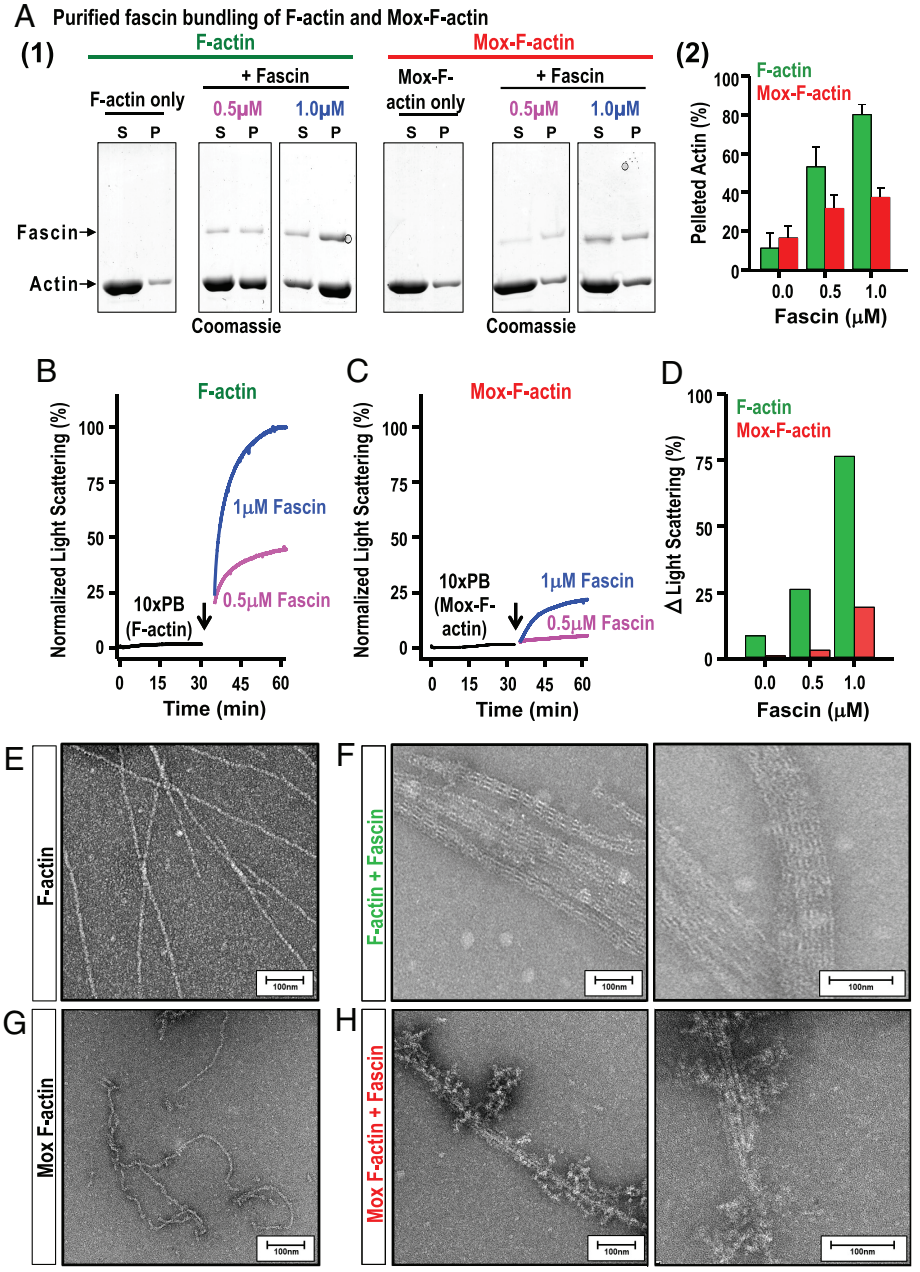

Fig. 2. Fascin poorly bundles Mical-oxidized F-actin. (*A*) Low-speed pelleting. (1) Supernatant (S) and pellet (P) contents of F-actin and Mox-F-actin incubated without or with fascin. (2) Pelleted F-actin and Mox-F-actin percentage at different [fascin]. [actins] = 5 μM, [fascin] = see figure. Representative experiments are shown. n = 3 independent experiments/condition. Mean ± SEM. (*B–D*) Light scattering assays. Black trace = actin polymerization using a 10×-concentrated polymerization buffer (PB). Black arrow=fascin addition. [fascin] = see figure. Representative experiments are shown. n = 3 independent experiments/condition. (*E–H*) Transmission EM images of negatively stained F-actin alone (*E*), F-actin with fascin (*F*), Mox-F-actin alone (*G*), and Mox-F-actin with fascin (*H*) reveal that unmodified F-actin bundles are smooth and coherent while Mox-F-actin forms short, coarse, and disordered bundles. (*F* and *H*) low (*Left*) and high (*Right*) image magnification.

Mical's NADPH consumption activity (Fig. 3*A*, compare blue and red traces, *SI Appendix*, Fig. S3 *A* and *B*, compare green and red traces). Yet, since we did not observe any difference in Mical's binding to fascin-bundled F-actin versus unbundled F-actin (*SI Appendix*, Fig. S3*D*), these results suggested that fascin's presence in bundled F-actin decreases Mical's enzymatic action on F-actin. Indeed, both limited subtilisin assays and the actin^{MetO44} antibody revealed that fascin's presence reduced the efficiency of Mical's F-actin oxidation (Fig. 3 *C* and *D*). Likewise, pyrene fluorescence assays revealed that Mical's disassembly of bundled F-actin was ~10% slower than its disassembly of unbundled F-actin (Fig. 3*E*). Furthermore, our TIRFM assays confirmed that F-actin bundles (blue arrowheads) persisted longer than unbundled filaments (red arrowheads) upon their Mical/NADPH-mediated oxidation [Fig. 1*E* (1 and 2)]. Employing TIRFM movies to measure the average decrease in fluorescence signal (Alexa488-SE) per square micron over time (0 to 400 sec (s)) also revealed a slower decay of fluorescence signal in the Mical/NADPH-treated fascin-bundled versus unbundled F-actin samples (Fig. 3*F*). Likewise, measuring the shrinkage rates of individual fascin-bundled filaments (blue dots) versus single unbundled filaments (red dots) upon Mical/NADPH treatment showed that the shrinkage rates of fascin-bundled filaments were (on average) 8.5-fold slower than those of unbundled filaments [0.9 ± 0.6 μm/min (n = 41) versus 7.44

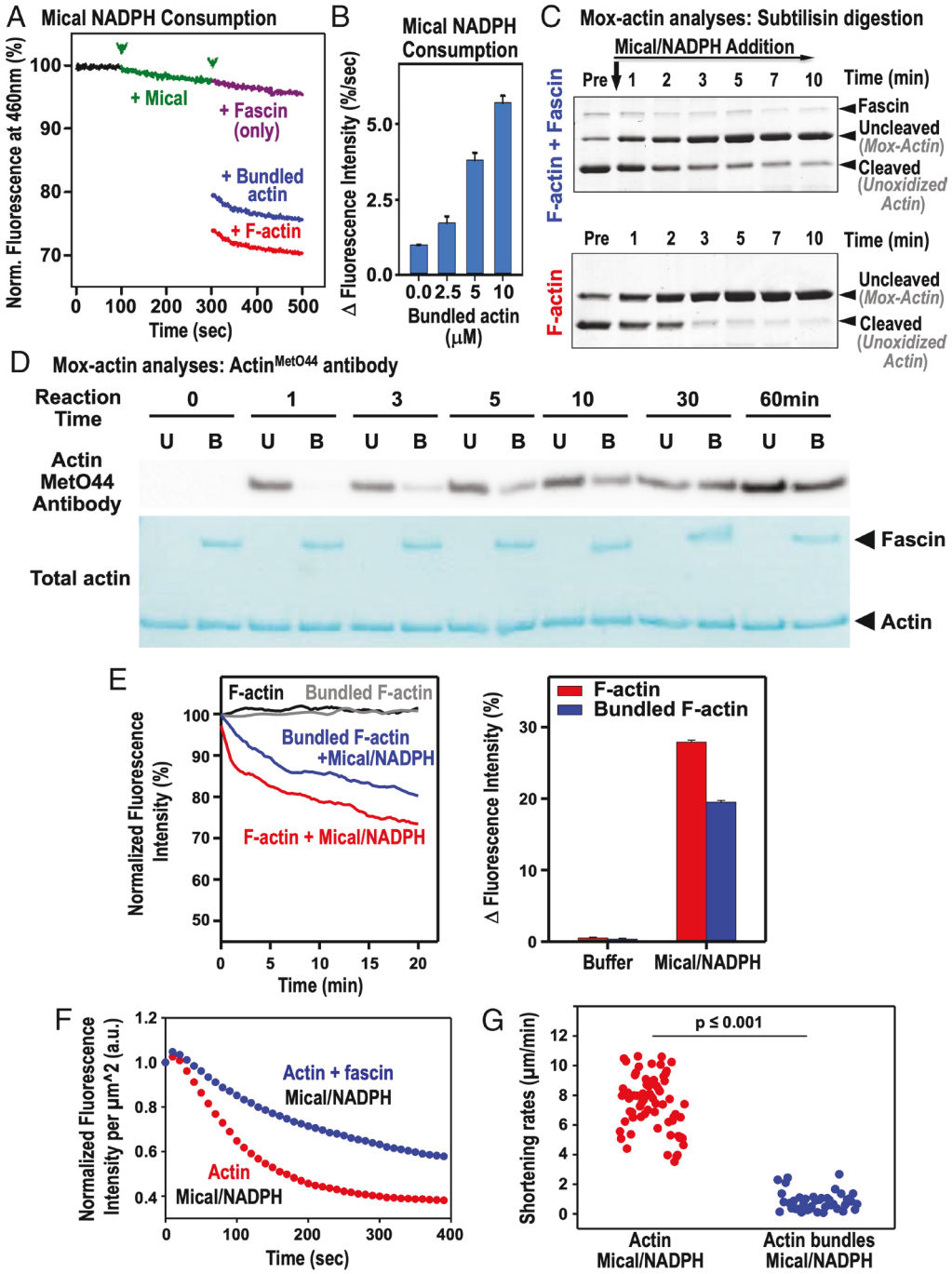

Fig. 3. Fascin-bundling regulates Mical's oxidation-mediated F-actin disassembly activity. (*A* and *B*) Mical's enzymatic activity, as judged by NADPH consumption [conversion of NADPH to NADP+ (fluorescence decrease/change)] is activated by fascin-bundled F-actin but to a lesser extent than by unbundled F-actin. A = [F-actin] = 2.5 μM, [fascin] = 0.5 μM, [Mical] = 0.6 μM, [NADPH] = 200 μM. B = Mical's increasing enzymatic activity with increasing [fascin-bundled F-actin]. n = 3 independent experiments/condition, mean ± SEM. (*C* and *D*) Mical oxidizes F-actin bundled by fascin, but at a slower rate than unbundled F-actin. (*C*) Subtilisin does not cleave Mical-oxidized actin between its M47 and G48 residues (24, 25). (*Upper*) Mical/NADPH's addition decreases subtilisin's cleavage of fascin-bundled F-actin over time. This reveals Mical/NADPH oxidizes fascin-bundled F-actin. (*Lower*) Mical/NADPH's addition more rapidly decreases subtilisin's cleavage of unbundled versus bundled F-actin (compare Cleaved Actin, *Lower* and *Upper*). This reveals fascin's presence dampens Mical-mediated F-actin oxidation. Pre = prior to Mical/NADPH addition (note that a small amount of actin is not cleaved under our conditions even without Mical/NADPH present). [F-actin] = 3.5 μM, [fascin] = 0.7 μM, [Mical] = 0.01 μM, and [NADPH] = 100 μM. (*D*) Actin^{MetO44}-specific antibody shows that Mical oxidizes fascin-bundled F-actin (B lanes), but this oxidation is slower than that seen with unbundled F-actin (U lanes). [F-actin] = 1.15 μM, [fascin] = 0.5 μM, [Mical] = 0.05 μM, and [NADPH] = 100 μM. (*E–G*) Fascin-bundling slows Mical's F-actin disassembly. (*E*) Pyrene-actin fluorescence (407 nm) assay. [F-actin] = 2.5 μM, [cofilin] = 0.25 μM, [Mical] = 0.025 μM, and [NADPH] = 100 μM. Representative experiment, n = 3 independent experiments/condition, mean ± SEM. (*F*) Average fluorescence intensities/μm^2 for TIRFM movies reveal Mical/NADPH induces a ~twofold slower fluorescence signal decay in fascin-bundled F-actin (blue) compared to unbundled filaments (red). Data averaged from four movies. n = 3 separate experiments. (*G*) Shortening rate measurements show a statistically significant (8.5-fold) inhibition of Mical-mediated disassembly by fascin-bundled F-actin (n = 41, blue) compared to unbundled filaments (n = 66, red). Mann–Whitney test. Measurements from three separate experiments. [actin] = 1.24 μM, [fascin] = 0.8 μM, [Mical] = 10 nM, and [NADPH] = 100 μM.

± 1.86 μm/min (n = 66), respectively] (Fig. 3*G*). Thus, fascin-induced bundling helps protect filaments from Mical-induced disassembly—which can be explained by the inhibition of both Mical's activation and its actin oxidation.

Mical Synergizes with Cofilin in Disassembly of Fascin-Bundled F-actin. To better define the mechanisms of bundled F-actin disassembly, we investigated the action of cofilin, which also disassembles fascin-bundled F-actin (13). Consistent with previous

results (13), we found that cofilin disassembled fascin-bundled F-actin (Fig. 4 and *SI Appendix*, Fig. S3 *E–I*). Yet, using light scattering assays to compare Mical to cofilin's effects revealed that Mical disassembled bundled F-actin more effectively—e.g., even at ~50-fold reduced levels [compare Fig. 1*D*, blue (Mical = 0.05 μM) and *SI Appendix*, Fig. S3*I*, magenta (cofilin = 2.5 μM)]. Notably, Mical and cofilin have been found to synergistically disassemble unbundled F-actin (i.e., when added together they are more effective at disassembling unbundled F-actin than the sum of their individual effects) (10, 24, 27). We therefore explored Mical and cofilin's combined effects on fascin-bundled F-actin. Notably, we did not observe any decreased ability of Mical to bind to fascin-bundled F-actin in the presence of different cofilin concentrations (*SI Appendix*, Fig. S3*J*). Indeed, pyrene-actin, light scattering,

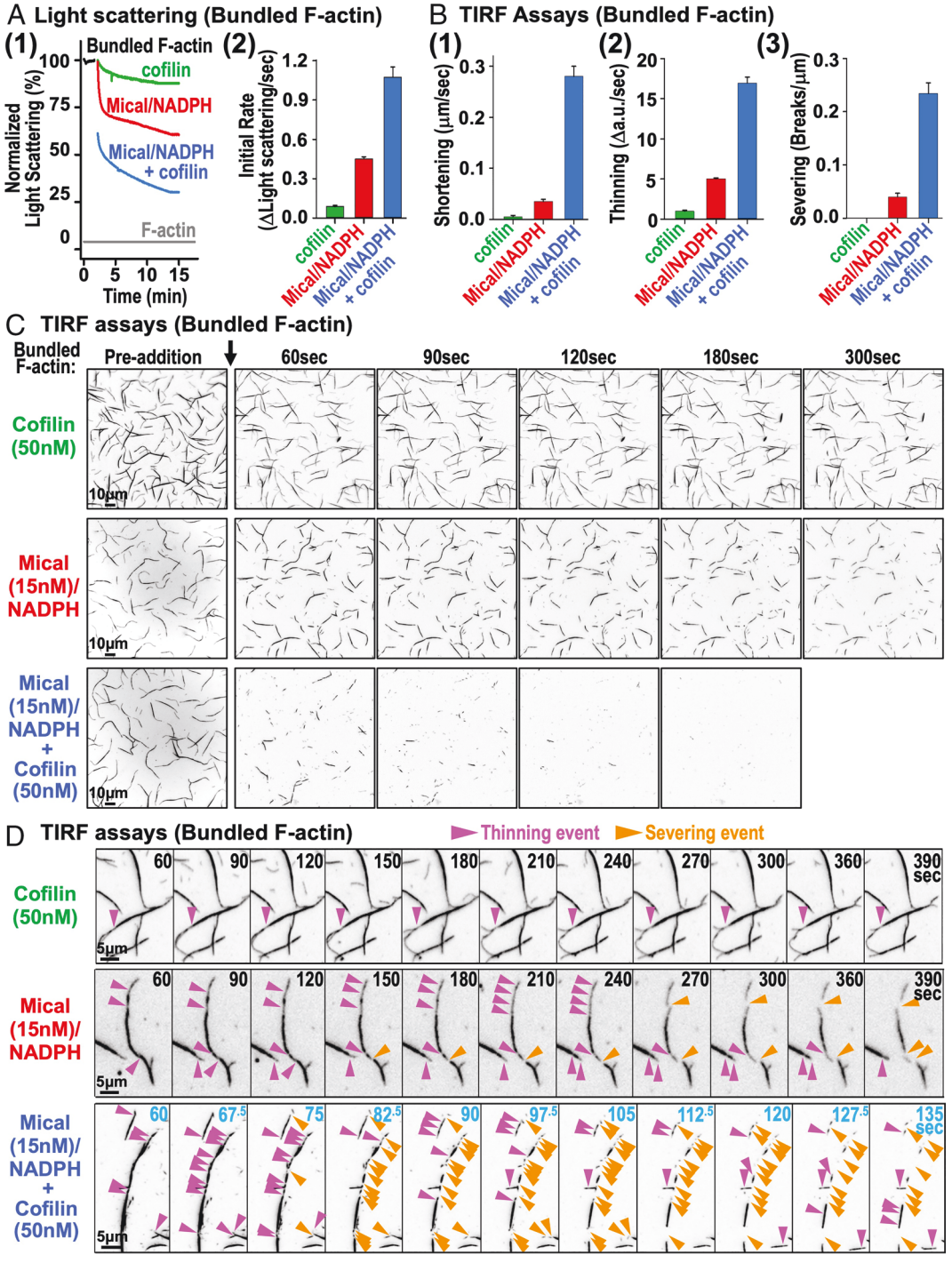

Fig. 4. Mical synergizes with cofilin to enhance fascin-bundled F-actin disassembly. Light scattering (*A*) and TIRF assays (*B–D*) reveal that together Mical and cofilin disassemble bundled F-actin more rapidly and more effectively than the sum of separate cofilin and Mical disassembly rates. (*A*) Light scattering: Graphs show the changes (1) and the initial rates of change (2). [actin] = 5 μM; [fascin] = 1 μM; [cofilin] = 1 μM; [Mical] = 0.05 μM; and [NADPH] = 100 μM. A representative experiment is shown; n = 5. Mean ± SEM. (*B*) TIRF assays: graphs show the rates of bundles shortening (1), thinning (2), and severing (3) from experiments described in *C* and *D* (data are averaged from five different movies). n = 40, 27, and 35 bundles used for Mical, cofilin, and both Mical and cofilin conditions, respectively. Mean ± SEM. (*C* and *D*) Representative time-lapse TIRFM video montages of fascin-bundled F-actin disassembly in the presence of cofilin, Mical, and Mical + cofilin (arrow = addition of each). Note the shortened time frame in Mical + cofilin in *D*. [actin] = 1 μM, 20% Alexa labeled; [fascin] = 1 μM; [cofilin] = 50 nM; [Mical] = 15 nM; and [NADPH] = 100 μM.

and TIRF assays revealed that Mical and cofilin synergize to disassemble bundled F-actin (Fig. 4 and *SI Appendix*, Fig. S3 *E–G*). For example, using TIRF assays, we found that at low (50 nM) concentrations, cofilin only minimally affected F-actin bundles (Fig. 4 *B* and *C* and Movie S4). Low concentrations of Mical (15 nM), while more effective than cofilin at disassembling F-actin bundles, did not completely disassemble them within 300 s (Fig. 4 *B* and *C* and Movie S5). Strikingly, adding both Mical and cofilin together resulted in rapid and extensive bundles disassembly, with their remnants gone within 180 s (Fig. 4 *B* and *C* and Movie S6). Moreover, our analyses revealed that cofilin alone induced only slight shortening and thinning, but no severing of bundles within 300 s (Fig. 4 *B* and *D*, pink arrows). Mical alone induced more shortening and thinning of bundles (Fig. 4 *B* and *D*, and see also Fig. 1 *E–G*), and these thinning sites (Fig. 4*D*, pink arrows) became places where bundle severing could be observed over time (Fig. 4*D*, orange arrows). Adding both Mical and cofilin together dramatically enhanced the rate and number of bundles shortening, thinning, and severing events [Fig. 4 *B* and *D* (and note the different times scales in the different conditions in *D*)]. In this example, severing was observed after 15 s when Mical and cofilin were both present (Fig. 4*D*, Time = 75 s, orange arrows), but not until 90 s when Mical alone was present (Fig. 4*D*, Time = 150 s, orange arrows), and not at all when cofilin alone was present (Fig. 4*D*). Thus, Mical and cofilin form a synergistic "pair" to robustly disassemble fascin-bundled F-actin (*SI Appendix*, Fig. S3*K*).

Mical, in a Cofilin-Dependent Manner, Decreases Bundled F-actin In Vivo, Mimicking *Bundling Protein* Knockout Mutants. To further explore mechanisms of F-actin disassembly, we turned to the Drosophila bristle cell system because it is a high-resolution model for defining effects on both unbundled and bundled F-actin in vivo (Fig. 5*A* and ref. 28). Cofilin plays an important role in disassembling unbundled F-actin in bristles (29), but its role in disassembling bundled F-actin in them is less clear. Indeed, since bundled F-actin decreases (not increases) in bristles in *cofilin*$^{-/-}$ mutants (29), previous work indicates that cofilin provides G-actin to promote bundled F-actin assembly versus disassembling bundled F-actin in bristles in vivo. We therefore sought to use the bristle model to examine Mical and cofilin's combined effects on both unbundled and bundled F-actin in vivo. In particular, unbundled F-actin in bristles is organized into snarls/patches [Fig. 5*A* (1 and 2) and ref. 28], and we found that decreasing *Mical* levels increased unbundled F-actin snarls/patches, while increasing *Mical* levels, in a cofilin-dependent manner, decreased them (Fig. 5*B* and *SI Appendix*, Fig. S4*A*). These results are consistent with both Mical and cofilin's combined ability to disassemble unbundled F-actin in bristles (24, 29). Next, we examined Mical and cofilin's ability to disassemble bundled F-actin in bristles, which are prominently crosslinked together with fascin [Fig. 5*A* (1, 3) and refs. 21, 28, and 30]. Notably, we found that Mical and cofilin combine to extensively disassemble bundled F-actin in vivo (Fig. 5 *C–E*).

We next reasoned that if Mical is a major trigger for disassembling bundled F-actin in vivo, then increasing Mical should generate changes in bundled F-actin and cellular shape that resemble the effects of decreasing bundling proteins. However, previous results indicated that increasing Mical resulted in some similarities to removal/loss of bundling proteins, i.e., a decrease in parallel bundled F-actin (*SI Appendix*, Fig. S4*B* and ref. 8), but we also saw differences between these two manipulations, including Mical-induced F-actin branching (*SI Appendix*, Fig. S4*B* and ref. 8). Given our results with purified proteins—that Mical's F-actin disassembly ability is dampened by bundled F-actin (Fig. 3)—we reasoned that bundling proteins may be dampening Mical's effects also in vivo. This could explain why low-level (x1) Mical overexpression does not mimic the loss of bundling proteins. Compellingly, brightfield, confocal, and electron microscopy observations revealed that expressing higher (x2) in vivo levels of Mical [using the same highly active form of Mical (Mical^{RedoxCH}) used for our purified protein experiments] generated a loss of bundled F-actin and cellular shape changes that were notably similar to those by *bundling protein* –/– mutants (Fig. 5 *F–H* and *SI Appendix*, Fig. S4 *B–G*). Thus, our results indicate that Mical, in combination with cofilin, disassembles bundled F-actin in vivo.

Actin-Bundling Proteins Regulate Mical's Effects on F-actin/Cellular Remodeling In Vivo and Vice Versa. While our results support the point that Mical disassembles bundled F-actin in vivo, the dosage-sensitive nature (i.e., x2 versus x1 copies of Mical) of these effects suggests that actin-bundling proteins may be dampening Mical's effects in vivo. To further test this possibility, we turned to classical genetic interaction analyses where we could use specific mutants to increase or decrease the levels of bundling proteins in vivo and examine their effects on Mical-triggered bundled F-actin disassembly. Notably, we found that similar to what we observed with purified proteins, even small increases in *bundling proteins* in vivo (which do not have any observable defects on their own) decreased Mical's in vivo effects (*SI Appendix*, Fig. S5*A*). So too, even small decreases in bundling protein levels in vivo [using *bundling protein* heterozygous (+/–) mutants, which have no defects on their own], significantly increased Mical's in vivo effects (*SI Appendix*, Fig. S5*B*). Moreover, further decreasing *bundling protein* levels in vivo (using hypomorphic alleles to decrease but not eliminate bundling proteins) further increased Mical's effects in vivo (Fig. 5 *I* and *J* and *SI Appendix*, Fig. S5*C*). For example, compared to either increasing *Mical* (x1) or decreasing *bundlers* on their own, increasing *Mical* (x1) in combination with decreasing *bundlers* generated a 30 to 40% reduction in bundled F-actin, little elongated cellular structure, and a significant increase in bristle width that resembled the rounded shape of a cell body/leading edge of a cell (Fig. 5 *I* and *J* and *SI Appendix*, Fig. S5*C*). Last, we also observed the reciprocal effects: 1) that expressing higher levels of *bundling proteins* alone in vivo generated defects that looked similar to *Mical*$^{-/-}$-like in vivo defects (*SI Appendix*, Figs. S4*F* and S5*D*) and 2) even small decreases in *Mical* levels in vivo [using *Mical* heterozygous (+/–) mutants, which have no defects on their own] enhanced bundling protein effects (*SI Appendix*, Fig. S5*E*). Thus, our results indicate that Mical and actin-bundling proteins work in a fine-tuned antagonistic manner to regulate the stability of the actin cytoskeleton and dictate cell shape (*SI Appendix*, Fig. S5*F*).

Semaphorin/Plexin/Mical Repulsion Counteracts Actin-Bundling Proteins to Direct Axon Guidance. Both MICALs and actin-bundling proteins including fascin are expressed in developing neurons and regulate their morphology and growth (6, 7, 31–36). We therefore wondered whether a similar interplay between MICALs and actin-bundling proteins directs axon guidance in vivo. Employing as a model the stereotypic guidance pattern of Drosophila embryonic axons [Fig. 6*A* (1) and *SI Appendix*, Fig. S6*A*], we found that decreasing bundling protein levels resulted in prominent motor and CNS axon guidance defects [Fig. 6*A* (2 and 3) and *SI Appendix*, Fig. S6*B*]. These results provide a demonstration that actin-bundling proteins such as fascin, which are well-known to be expressed in the growth cones of navigating axons, are required for axon

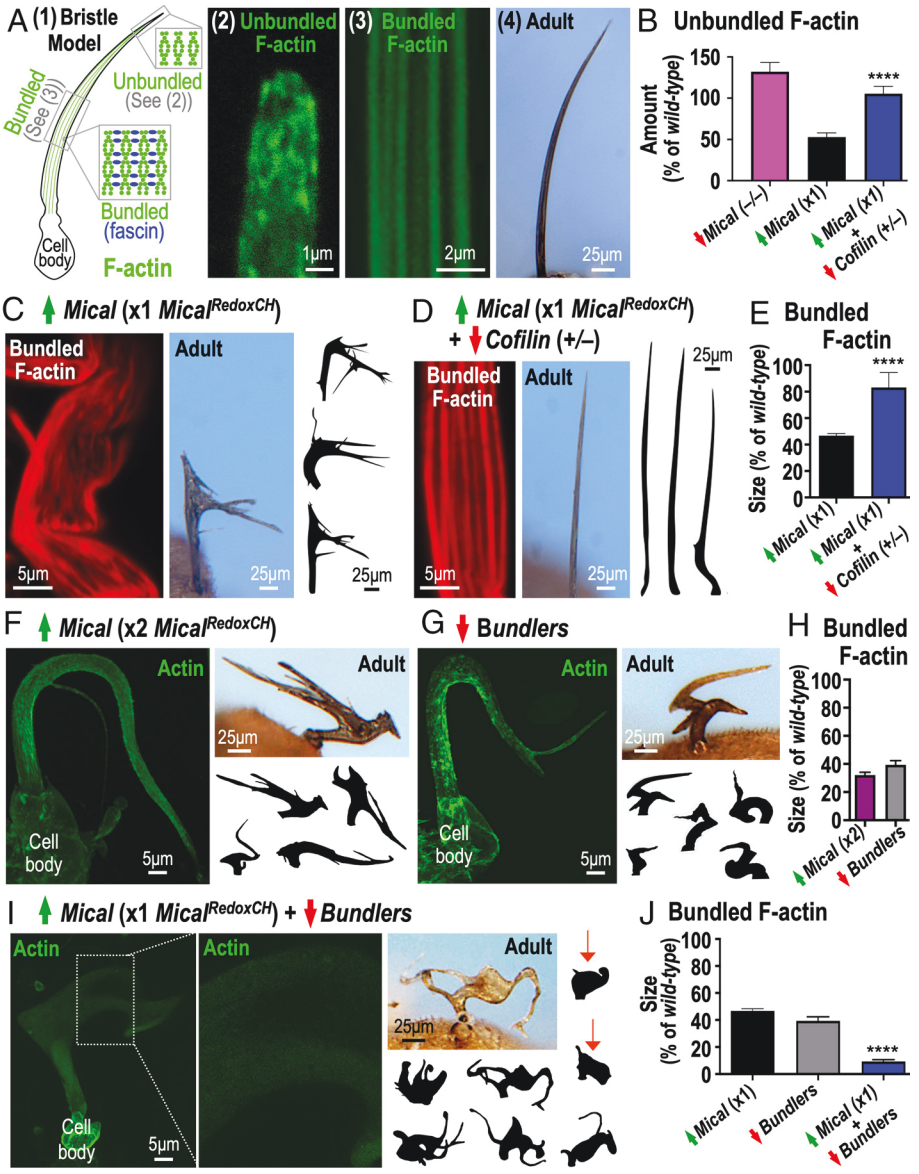

Fig. 5. Mical combines with cofilin to decrease bundled F-actin in vivo, but bundling proteins regulate this ability. (*A*) Bristle actin filaments (green) exist as both unbundled snarls/patches ((1) upper boxed region, (2)) and bundled F-actin ((1) lower boxed regions, (3)) crosslinked with bundling proteins (blue) to "push-out" long, branchless bristles (1 and 4). (*B*) Decreasing Mical in vivo increases unbundled F-actin and increasing Mical in vivo decreases unbundled F-actin in a cofilin-dependent manner. See *SI Appendix*, Fig. S4*A* for images. (*C*–*E*) Increasing Mical (*C* and *E*) in a cofilin-dependent manner (*D* and *E*) decreases bundled F-actin in bristles in vivo. (*F*–*H*) Increasing Mical to high levels (x2) in vivo (*F* and *H*) mimics the cellular and F-actin effects of decreasing bundling proteins in vivo (*G* and *H*). (*I* and *J*) Increasing Mical (x1) in combination with decreasing bundling proteins enhances the in vivo loss of bundled F-actin (green in *I*, and compare to altering either effector on its own in *J*) and generates bristles that have a rounded, cell-body-like shape (Adult, e.g., arrows). The dashed rectangular region is magnified in the adjacent image. Mean ± SEM for graphs, ****$P < 0.0001$, unpaired *t* test (two tailed) for *B*, *E*, and *J*.

guidance in vivo. Furthermore, similar to the reciprocal effects we observed between Mical and bundling proteins in the bristle system (Fig. 5 *F*–*H* and *SI Appendix*, Fig. S4 *E*–*G*), the types of guidance defects seen with decreased *bundling proteins* resembled those seen with increased *Mical* [Fig. 6*A* (2) and *SI Appendix*, Fig. S6 *C* and *D*, and refs. 8, 25, and 37]. In particular, similar to the increased axon–axon repulsion that occurs with neuronal Mical overexpression, we observed that *bundling protein (–/–)* mutant ISNb and SNa motor axons were often abnormally separated/defasciculated and did not navigate to their target areas [Fig. 6*A* (2) and *SI Appendix*, Fig. S6 *C* and *D*]. Likewise, CNS axons were also abnormally defasciculated in *bundling protein (–/–)* mutants, generating a Mical neuronal overexpression-like paucity of axons within fascicles and abnormal crossing between them [Fig. 6*A* (2)].

In light of these observations, and the antagonistic interactions we observed between Mical and actin-bundling proteins in affecting the shape and extension of the bristle cell model, we wondered whether similar interactions underlie axon guidance. Using Drosophila CNS axons as a model, we found that decreasing actin-bundling proteins significantly enhanced Mical neuronal overexpression guidance defects [Fig. 6*B* (1)]. These results support our work with purified proteins, the in vivo bristle model, and mutant analyses of axon guidance. They indicate that Mical and actin-bundling proteins counteract each other to guide axons. Interestingly, previous studies implicate the regulation of fascin/fascin-bundled F-actin as being important for neuronal growth cone retraction in response to repellents, including proNGF and semaphorins (38, 39). Since Mical is a Semaphorin (Sema) repulsive signaling component (*SI Appendix*, Fig. S6*E* and refs. 7 and 37), we wondered whether actin-bundling proteins play

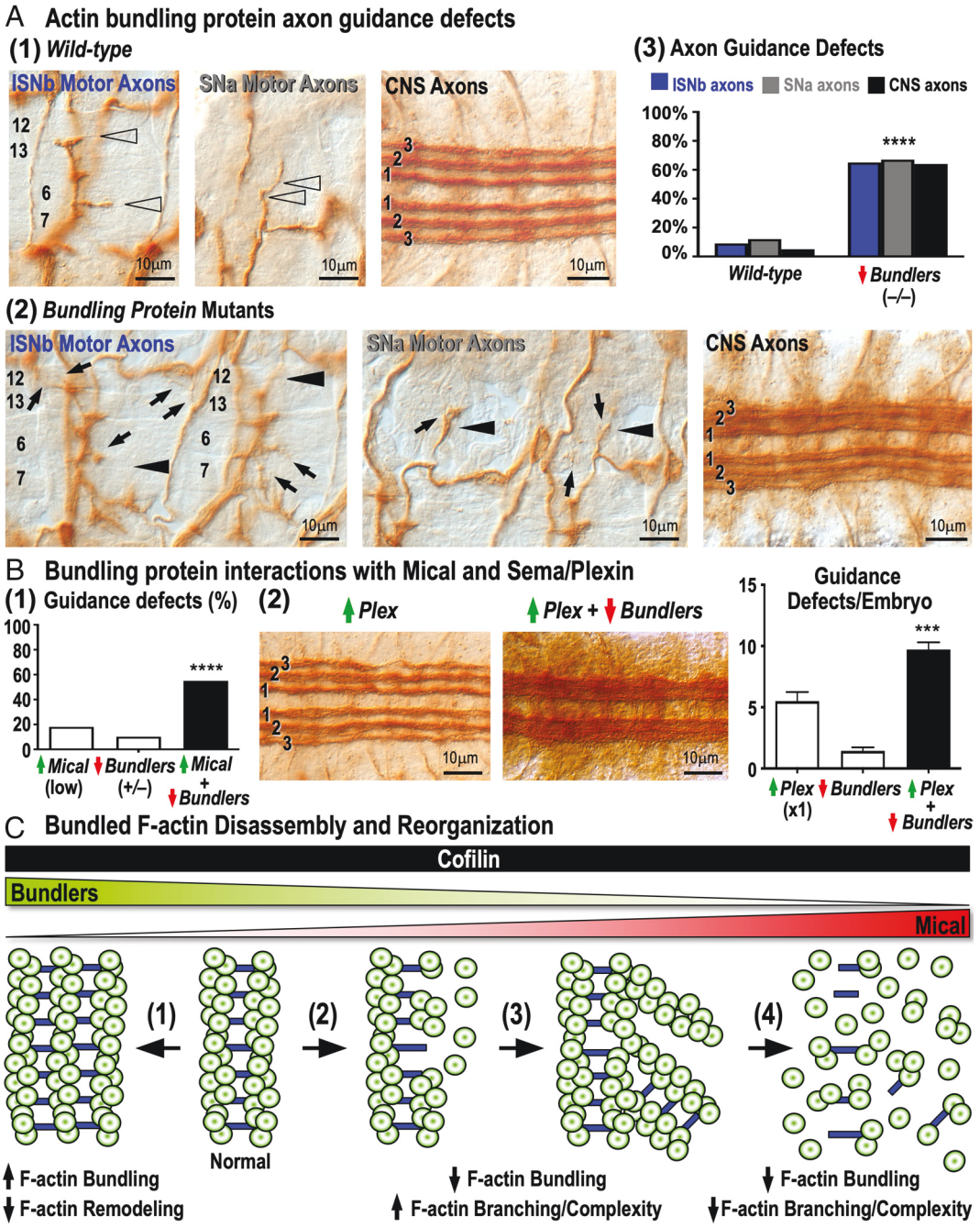

Fig. 6. Semaphorin/Plexin/Mical repulsion counteracts actin-bundling proteins to direct axon guidance. (*A*) *Bundling protein* knockout (–/–) mutants have axon guidance defects. (1) *Wild-type*: ISNb axons innervate muscles 6/7 and 12/13 (arrowheads), SNa axons make two easily-observable turns (arrowheads), and CNS axons project within three (1,2,3) equally-spaced/similar-width longitudinal fascicles. (2) *Bundling protein* mutant axons exhibit defects in innervating their targets (ISNb, arrowheads), making their two characteristic turns (SNa, arrowheads), and navigating within their three separate (1,2,3) longitudinal fascicles (CNS). Further, ISNb and SNa axons project excessively within the periphery/past their muscle targets (arrows) and CNS axons project abnormally between their three longitudinal fascicles. (3) Percentage (%) of ISNb, SNa, and CNS guidance defects. n≥96 hemisegments (10 animals/genotype). ****$P < 0.0001$; Chi-squared test. (*B*) Decreasing bundling proteins enhances increased neuronal Mical (1) and Plex (2) guidance defects. (2) Note, for example, that the three separate (1,2,3) longitudinal fascicles that are relatively weakly affected by Plex (Image, increasing Plex), are strongly affected and no longer easily discernable when increasing Plex is combined with decreasing bundling proteins (Image, increasing Plex + decreasing bundlers). n ≥ 100 hemisegments (10 animals/genotype). ****$P < 0.0001$, Chi-squared test. Mean ± SEM, ***$P < 0.001$, one-way ANOVA, Tukey's multiple comparison test. (*C*) Working model: Mical and actin-bundling proteins antagonize each other's actions to regulate F-actin network stability. When steady-state levels of cofilin are maintained, increasing Mical activity increases bundled F-actin disassembly: which at low levels increases F-actin/cellular remodeling and complexity in vivo (2 and 3) but at high levels decreases F-actin/cellular complexity (4). Lowering bundling proteins levels makes cells more susceptible to lower Mical levels (3 and 4), while increasing bundling proteins helps protect against Mical's effects—but also reduces F-actin/cellular remodeling (1).

a role in counteracting Sema-mediated repulsive axon guidance. To test for this, we employed an in vivo assay used to identify factors involved in repulsive axon guidance mediated by Semas and their Plexin (Plex) receptors. In particular, increasing neuronal Plex in vivo results in Sema-dependent increased axon-axon repulsion between typically adhered together (fasciculated) CNS axons [Fig. 6 *B* (2), *left* image, graph; (24, 25, 40)]. Notably, decreasing actin-bundling proteins significantly enhanced this Sema/Plexin-mediated axon-axon repulsion, such that in the most severe cases it was difficult to see any fasciculated longitudinal CNS axons [Fig. 6 *B* (2), *right* image,

graph]. Thus, our results show that Sema/Plex/Mical-mediated repulsive axon guidance antagonizes actin bundling protein effects in vivo—results that are also consistent with our observations using purified Mical, purified Mical-oxidized actin, and the in vivo bristle model.

Discussion

Disassembling stable higher-order bundled F-actin structures is necessary for numerous cellular behaviors and adaptations including division, growth, motility, navigation, connectivity, and plasticity. We now find that Mical rapidly and extensively disassembles filaments bundled together with one of the most prominent and widely-expressed crosslinking proteins, fascin. Namely, our results reveal that Mical is activated by fascin-bundled actin filaments to oxidize actin's M44 and M47 within them. This posttranslational effect not only disassembles fascin-bundled F-actin but also generates Mical-oxidized actin that is poorly bundled by fascin. Furthermore, previous observations revealed that cofilin preferentially affects immobilized/crosslinked filaments and that it cooperates with fascin to disassemble bundles (13, 41, 42). Our results now show that Mical greatly amplifies these cofilin effects and vice versa, resulting in their synergistic enhancement of fascin-bundled F-actin disassembly compared to that of the sum of both effectors alone. Similar Mical and cofilin-dependent disassembly effects on bundled F-actin also occur in vivo to allow for cellular growth, remodeling, guidance, and connectivity.

Our results also provide important insights into mechanisms governing bundled F-actin disassembly. In particular, fascin-mediated bundling dampens Mical-mediated actin oxidation and disassembly. We speculate that this effect can be explained in part by decreased accessibility of individual F-actins in the core of a bundle to Mical. Yet, several factors that are dependent on Mical's mechanisms of action counteract this reduced ability to oxidize actin bundles, resulting in their effective disassembly in vivo and in vitro (*SI Appendix*, Fig. S3*K*). Specifically, Mical-induced actin oxidation decreases fascin's ability to bundle filaments (including into tight arrays) as revealed by light scattering, low-speed pelleting, and EM experiments and supported by the detection of a "thinning/peeling mode" of bundles' disassembly. This suggests that in a preformed bundle (as found in vivo), such weakening of fascin bundling would gradually increase the accessibility of the bundle's core to Mical binding and hence facilitate Mical's oxidation of actin. In line with this, our analysis of the data in Fig. 3*G* showed that thinner bundles (~3 filaments on average) shorten faster (1.07 ± 0.67 μm/min) compared to the thicker bundles (~5 filaments average, 0.64 ± 0.5 μm/min). Additionally, previous studies showed that MICALs' oxidation of F-actin combines with improved cofilin binding to Mox-F-actin (compared to unoxidized F-actin) to provide an effective mechanism for F-actin disassembly in its different nucleotide-bound states (both ADP- and ADP-Pi-bound) (10, 24, 27). We propose that susceptibility of fascin-bundles to cofilin-mediated disassembly (13) synergizes with the improved cofilin binding to Mox-F-actin (10, 24, 27), and Mox-F-actin's sensitivity to cofilin's actions (10, 24, 27), to drive enhanced bundle dismantling. These results also provide a foundation for future work investigating whether other types of bundled F-actin networks (i.e., those assembled by other crosslinking proteins and/or combinations of them with each other or with fascin) might be more or less resistant to Mical or Mical in combination with cofilin. Likewise, since bundling proteins (such as fascin) are under transcriptional and posttranslational regulation (19, 20, 22, 23), future work should investigate whether Mical's activation might combine with such bundling proteins regulation.

F-actin bundles have been linked to supporting the directed migration/guidance of migrating cells and neuronal growth cones (43, 44). So too, extracellular cues such as growth factors and thrombospondin, that are supportive of growth and migration, have been linked to increasing fascin-bundled F-actin (19), while repulsive guidance cues such as Semas and proNGF exert their negative effects on growth, guidance, and migration by disrupting fascin-bundled F-actin (38, 39, 45). Our observations now provide mechanisms underlying the repellent-driven breakdown of fascin-bundled filaments. In addition, previous work has revealed that repellent-driven F-actin disassembly often leads to less cellular complexity, but paradoxically, it can also induce more branching/plasticity/complexity (e.g., refs. 8, 25, and 46–51). Our results now mechanistically explain these previous observations. In particular, we find that low levels of repulsive signaling induce more actin network complexity [Fig. 6*C* (2 and 3)]. In contrast, high levels of repulsive signaling prevent this plasticity and disassemble F-actin to the point that is detrimental to normal cellular shape and extension [Fig. 6*C* (4) and *SI Appendix*, Fig. S5*F*]. Bundled F-actin helps control these effects, including helping to safeguard against Mical-triggered F-actin disassembly and remodeling [Fig. 6*C* (1 to 4)]. Thus, our results indicate that cells need to tightly control repulsive signaling in order to fine-tune the organization of the cytoskeleton—and some of this can be accomplished via an interplay of F-actin crosslinking by fascin and its dampening of Mical and cofilin's effects.

It is notable that high levels of F-actin-bundling proteins can reduce cellular remodeling and are detrimental to normal cellular shape and extension [Fig. 6*C* (1)]. Changes to fascin levels, in particular, have been linked to numerous pathologies including neurological abnormalities such as retinal degeneration, seizures, and hearing loss (19, 22, 52). Fascin's link to hearing loss is particularly interesting given that it is highly expressed in stereocilia of sound-transducing inner ear hair cells (52), a mechanosensory apparatus that has structural and functional analogies to the Drosophila bristle (53). Interestingly, MICALs have also been prominently linked to neurological deficits including epilepsy (7). Mical—through its role in the neurosensory bristle and its interactions with other proteins required for hearing, including Myosin15 and MsrB/SelR (8, 12, 52, 54),—has also been associated with mechanosensation. So too, elevated fascin level is prominently associated with many human cancer types—as it induces abnormal cellular growth, stiffness, movement, and invasiveness—and is correlated with aggressive clinical progression, poor prognosis, and high mortality (23, 55, 56). For these reasons, fascin has garnered considerable recent attention as a candidate biomarker for multiple cancer types and a potential therapeutic target (23, 56–58). Given our observations of mechanisms to disassemble fascin-bundled filaments, and that MICAL family proteins have also been found to regulate the mobility, metastasis, and invasion of different cancer cells (6, 7), future work should explore the interactions between Mical and fascin-bundled F-actin in therapeutic contexts.

Materials and Methods (see also *SI Appendix, Extended Methods*)

Protein purification, labeling, subtilisin digestions, pelleting, disassembly, trypsin digestion, NADPH consumption, TIRF microscopy/analyses, EM, and Actin^{MetO44} antibody assays were performed based on described methods (8–10, 24, 25). Light scattering was done using standard approaches. Flies, molecular biology, and genetic procedures were as reported (8, 24, 29, 40) except for actin bundler mutant stocks (Bloomington Drosophila Stock Center, Indiana,

USA), UAS:GFP-fascin stocks (kind gifts of S. Plaza ref. 36), *Mical*^{15256} (kind gift of F. Yu; ref. 59), and our UAS:Drosophila fascin (untagged) stocks. In vivo imaging, drawings, and analyses were done based on described approaches (8, 25, 37, 40, 60).

Data, Materials, and Software Availability. All study data are included in the article and/or supporting information. All study data, as well as all materials/reagents, are also available on request from the corresponding authors.

ACKNOWLEDGMENTS. We thank Terman, Reisler, and Grintsevich lab members for discussions. We also thank R.-J. Hung, B. Lee, J. Merriam, S. Plaza, F. Yu, and the Bloomington Stock Center for reagents and J. Rodriguez and M. Flores for help with imaging actin assemblies. Supported by grants: NSF CAREER 2146328 (E.E.G.), NIH GM077190 (E.R.), NIH NS073968 (J.R.T.), and Welch Foundation I-1749 (J.R.T.).

Author affiliations: [a]Department of Chemistry and Biochemistry, University of California, Los Angeles, CA 90095; [b]Department of Neuroscience, The University of Texas of Southwestern Medical Center, Dallas, TX 75390; [c]Department of Pharmacology, The University of Texas of Southwestern Medical Center, Dallas, TX 75390; [d]Department of Chemistry and Biochemistry, California State University, Long Beach, CA 90840; and [e]Molecular Biology Institute, University of California, Los Angeles, CA 90095

1. T. D. Pollard, Actin and actin-binding proteins. *Cold Spring Harb. Perspect. Biol.* **8**, a018226 (2016).
2. L. Blanchoin, R. Boujemaa-Paterski, C. Sykes, J. Plastino, Actin dynamics, architecture, and mechanics in cell motility. *Physiol. Rev.* **94**, 235–263 (2014).
3. S. Rajan, D. S. Kudryashov, E. Reisler, Actin bundles dynamics and architecture. *Biomolecules* **13**, 450 (2023).
4. T. Miyoshi, N. Watanabe, Can filament treadmilling alone account for the F-actin turnover in lamellipodia? *Cytoskeleton (Hoboken)* **70**, 179–190 (2013).
5. W. Brieher, Mechanisms of actin disassembly. *Mol. Biol. Cell* **24**, 2299–2302 (2013).
6. C. Rouyere, T. Serrano, S. Fremont, A. Echard, Oxidation and reduction of actin: Origin, impact in vitro and functional consequences in vivo. *Eur. J. Cell Biol.* **101**, 151249 (2022).
7. S. Rajan, J. R. Terman, E. Reisler, MICAL-mediated oxidation of actin and its effects on cytoskeletal and cellular dynamics. *Front. Cell Dev. Biol.* **11**, 1124202 (2023).
8. R. J. Hung *et al.*, Mical links semaphorins to F-actin disassembly. *Nature* **463**, 823–827 (2010).
9. R. J. Hung, C. W. Pak, J. R. Terman, Direct redox regulation of F-actin assembly and disassembly by Mical. *Science* **334**, 1710–1713 (2011).
10. E. E. Grintsevich *et al.*, Catastrophic disassembly of actin filaments via Mical-mediated oxidation. *Nat. Commun.* **8**, 2183 (2017).
11. H. Wu, H. G. Yesilyurt, J. Yoon, J. R. Terman, The MICALs are a family of F-actin dismantling oxidoreductases conserved from drosophila to humans. *Sci. Rep.* **8**, 937 (2018).
12. R. J. Hung, C. S. Spaeth, H. G. Yesilyurt, J. R. Terman, SelR reverses Mical-mediated oxidation of actin to regulate F-actin dynamics. *Nat. Cell Biol.* **15**, 1445–1454 (2013).
13. D. Breitsprecher *et al.*, Cofilin cooperates with fascin to disassemble filopodial actin filaments. *J. Cell Sci.* **124**, 3305–3318 (2011).
14. A. Michelot *et al.*, Actin-filament stochastic dynamics mediated by ADF/cofilin. *Curr Biol* **17**, 825–833 (2007).
15. K. M. Schmoller, C. Semmrich, A. R. Bausch, Slow down of actin depolymerization by cross-linking molecules. *J. Struct. Biol.* **173**, 350–357 (2011).
16. S. Huang *et al.*, Arabidopsis VILLIN1 generates actin filament cables that are resistant to depolymerization. *Plant Cell* **17**, 486–501 (2005).
17. N. Elkhatib *et al.*, Fascin plays a role in stress fiber organization and focal adhesion disassembly. *Curr. Biol.* **24**, 1492–1499 (2014).
18. H. Mizuno, K. Tanaka, S. Yamashiro, A. Narita, N. Watanabe, Helical rotation of the diaphanous-related formin mDia1 generates actin filaments resistant to cofilin. *Proc. Natl. Acad. Sci. U.S.A.* **115**, E5000–E5007 (2018).
19. Y. Hashimoto, D. J. Kim, J. C. Adams, The roles of fascins in health and disease. *J. Pathol.* **224**, 289–300 (2011).
20. A. Jayo, M. Parsons, Fascin: A key regulator of cytoskeletal dynamics. *Intern. J. Biochem. Cell Biol.* **42**, 1614–1617 (2010).
21. C. Revenu, R. Athman, S. Robine, D. Louvard, The co-workers of actin filaments: From cell structures to signals. *Nat. Rev. Mol. Cell Biol.* **5**, 635–646 (2004).
22. M. C. Lamb, T. L. Tootle, Fascin in cell migration: More than an actin bundling protein. *Biology (Basel)* **9**, 403 (2020).
23. S. Lin, M. D. Taylor, P. K. Singh, S. Yang, How does fascin promote cancer metastasis? *FEBS J.* **288**, 1434–1446 (2021).
24. E. E. Grintsevich *et al.*, F-actin dismantling through a redox-driven synergy between Mical and cofilin. *Nat. Cell Biol.* **18**, 876–885 (2016).
25. E. E. Grintsevich *et al.*, Profilin and Mical combine to impair F-actin assembly and promote disassembly and remodeling. *Nat. Commun.* **12**, 5542 (2021).
26. A. Muhlrad *et al.*, Cofilin induced conformational changes in F-actin expose subdomain 2 to proteolysis. *J. Mol. Biol.* **342**, 1559–1567 (2004).
27. H. Wioland *et al.*, Actin filament oxidation by MICAL1 suppresses protections from cofilin-induced disassembly. *EMBO Rep.* **22**, e50965 (2021).
28. L. G. Tilney, D. J. DeRosier, How to make a curved Drosophila bristle using straight actin bundles. *Proc. Natl. Acad. Sci. U.S.A.* **102**, 18785–18792 (2005).
29. J. Wu, H. Wang, X. Guo, J. Chen, Cofilin-mediated actin dynamics promotes actin bundle formation during Drosophila bristle development. *Mol. Biol. Cell* **27**, 2554–2564 (2016).
30. J. R. Bartles, Parallel actin bundles and their multiple actin-bundling proteins. *Curr. Opin. Cell Biol.* **12**, 72–78 (2000).
31. C. S. Cohan, E. A. Welnhofer, L. Zhao, F. Matsumura, S. Yamashiro, Role of the actin bundling protein fascin in growth cone morphogenesis: Localization in filopodia and lamellipodia. *Cell Motil. Cytoskeleton* **48**, 109–120 (2001).
32. R. Kraft *et al.*, Phenotypes of Drosophila brain neurons in primary culture reveal a role for fascin in neurite shape and trajectory. *J. Neurosci.* **26**, 8734–8747 (2006).
33. M. Nozumi, F. Nakatsu, K. Katoh, M. Igarashi, Coordinated movement of vesicles and actin bundles during nerve growth revealed by superresolution microscopy. *Cell Rep.* **18**, 2203–2216 (2017).
34. Z. Wei, M. Sun, X. Liu, J. Zhang, Y. Jin, Rufy3, a protein specifically expressed in neurons, interacts with actin-bundling protein Fascin to control the growth of axons. *J. Neurochem.* **130**, 678–692 (2014).
35. J. Nagel *et al.*, Fascin controls neuronal class-specific dendrite arbor morphology. *Development* **139**, 2999–3009 (2012).
36. J. Zanet *et al.*, Fascin is required for blood cell migration during Drosophila embryogenesis. *Development* **136**, 2557–2565 (2009).
37. J. R. Terman, T. Mao, R. J. Pasterkamp, H. H. Yu, A. L. Kolodkin, MICALs, a family of conserved flavoprotein oxidoreductases, function in plexin-mediated axonal repulsion. *Cell* **109**, 887–900 (2002).
38. J. A. Brown, P. C. Bridgman, Disruption of the cytoskeleton during Semaphorin 3A induced growth cone collapse correlates with differences in actin organization and associated binding proteins. *Dev. Neurobiol.* **69**, 633–646 (2009).
39. K. Deinhardt *et al.*, Neuronal growth cone retraction relies on proneurotrophin receptor signaling through Rac. *Sci. Signal* **4**, ra82 (2011).
40. T. Yang, J. R. Terman, 14-3-3epsilon couples protein kinase A to semaphorin signaling and silences plexin RasGAP-mediated axonal repulsion. *Neuron* **74**, 108–121 (2012).
41. D. Pavlov, A. Muhlrad, J. Cooper, M. Wear, E. Reisler, Actin filament severing by cofilin. *J. Mol. Biol.* **365**, 1350–1358 (2007).
42. H. Wioland, A. Jegou, G. Romet-Lemonne, Torsional stress generated by ADF/cofilin on cross-linked actin filaments boosts their severing. *Proc. Natl. Acad. Sci. U.S.A.* **116**, 2595–2602 (2019).
43. E. W. Dent, S. L. Gupton, F. B. Gertler, The growth cone cytoskeleton in axon outgrowth and guidance. *Cold Spring Harb. Perspect. Biol.* **3**, a001800 (2011).
44. S. SenGupta, C. A. Parent, J. E. Bear, The principles of directed cell migration. *Nat. Rev. Mol. Cell Biol.* **22**, 529–547 (2021).
45. X. Li, J. W. Law, A. Y. Lee, Semaphorin 5A and plexin-B3 regulate human glioma cell motility and morphology through Rac1 and the actin cytoskeleton. *Oncogene* **31**, 595–610 (2012).
46. J. P. Kapfhammer, J. A. Raper, Collapse of growth cone structure on contact with specific neurites in culture. *J. Neurosci.* **7**, 201–212 (1987).
47. D. S. Campbell *et al.*, Semaphorin 3A elicits stage-dependent collapse, turning, and branching in Xenopus retinal growth cones. *J. Neurosci.* **21**, 8538–8547 (2001).
48. V. Fenstermaker, Y. Chen, A. Ghosh, R. Yuste, Regulation of dendritic length and branching by semaphorin 3A. *J. Neurobiol.* **58**, 403–412 (2004).
49. Y. Liu, M. C. Halloran, Central and peripheral axon branches from one neuron are guided differentially by Semaphorin3D and transient axonal glycoprotein-1. *J. Neurosci.* **25**, 10556–10563 (2005).
50. J. A. Sakai, M. C. Halloran, Semaphorin 3d guides laterality of retinal ganglion cell projections in zebrafish. *Development* **133**, 1035–1044 (2006).
51. T. S. Tran, A. L. Kolodkin, R. Bharadwaj, Semaphorin regulation of cellular morphology. *Annu. Rev. Cell Dev. Biol.* **23**, 263–292 (2007).
52. A. C. Velez-Ortega, G. I. Frolenkov, Building and repairing the stereocilia cytoskeleton in mammalian auditory hair cells. *Hear Res.* **376**, 47–57 (2019).
53. U. Muller, A. Littlewood-Evans, Mechanisms that regulate mechanosensory hair cell differentiation. *Trends Cell Biol.* **11**, 334–342 (2001).
54. S. K. Rich, R. Baskar, J. R. Terman, Propagation of F-actin disassembly via Myosin15-Mical interactions. *Sci. Adv.* **7**, eabg0147 (2021).
55. R. P. Stevenson, D. Veltman, L. M. Machesky, Actin-bundling proteins in cancer progression at a glance. *J. Cell Sci.* **125**, 1073–1079 (2012).
56. H. Liu *et al.*, Fascin actin-bundling protein 1 in human cancer: Promising biomarker or therapeutic target? *Mol. Ther. Oncolytics* **20**, 240–264 (2021).
57. Y. Ma, L. M. Machesky, Fascin1 in carcinomas: Its regulation and prognostic value. *Int. J. Cancer* **137**, 2534–2544 (2015).
58. B. Ristic *et al.*, Emerging role of Fascin-1 in the pathogenesis, diagnosis, and treatment of the gastrointestinal cancers. *Cancers (Basel)* **13**, 2536 (2021).
59. D. Kirilly *et al.*, A genetic pathway composed of Sox14 and Mical governs severing of dendrites during pruning. *Nat. Neurosci.* **12**, 1497–1505 (2009).
60. J. Yoon, S. B. Kim, G. Ahmed, J. W. Shay, J. R. Terman, Amplification of F-Actin disassembly and cellular repulsion by growth factor signaling. *Dev. Cell* **42**, 117–129 (2017).